Plant Biotechnology Journal
Open Access

Plant Biotechnology Journal (2019) **17**, pp. 2313–2324 doi: 10.1111/pbi.13142

A novel quantitative trait locus on chromosome A9 controlling oleic acid content in *Brassica napus*

Qing Zhao[1,†], Jian Wu[1,a,†], Guangqin Cai[1], Qingyong Yang[2], Muhammad Shahid[1], Chuchuan Fan[1], Chunyu Zhang[1] and Yongming Zhou[1,*]

[1]*National Key Laboratory of Crop Genetic Improvement, Huazhong Agricultural University, Wuhan, Hubei, China*
[2]*Hubei Key Laboratory of Agricultural Bioinformatics, College of Informatics, Huazhong Agricultural University, Wuhan, Hubei, China*

Received 3 March 2019;
revised 24 April 2019;
accepted 26 April 2019.
**Correspondence* (Tel +86-27-87286869; fax +86-27-87280016; email ymzhou@mail.hzau.edu.cn)
[a]Present address: Jiangsu Provincial Key Laboratory of Crop Genetics and Physiology, Yangzhou University, Yangzhou, 225009, Jiangsu, China.
[†]These authors contributed equally to the work.

Keywords: rapeseed, oleic acid, quantitative trait loci.

Summary

One of the most important goals in the breeding of oilseed crops, including *Brassica napus*, is to improve the quality of edible vegetable oil, which is mainly determined by the seed fatty acid composition, particularly the C18:1 content. Previous studies have indicated that the C18:1 content is a polygenic trait, and no stable quantitative trait loci (QTLs) except for *FAD2* have been reported. By performing a GWAS using 375 low erucic acid *B. napus* accessions genotyped with the Brassica 60K SNP array and constructing a high-density SNP-based genetic map of a 150 DH population, we identified a novel QTL on the A9 chromosome. The novel locus could explain 11.25%, 5.72% and 6.29% of phenotypic variation during three consecutive seasons and increased the C18:1 content by approximately 3%–5%. By fine mapping and gene expression analysis, we found three potential candidate genes and verified the fatty acids in a homologous gene mutant of Arabidopsis. A metal ion-binding protein was found to be the most likely candidate gene in the region. Thus, the C18:1 content can be further increased to about 80% with this novel locus together with *FAD2* mutant allele without compromise of agronomic performance. A closely linked marker, BnA129, for this novel QTL (*OLEA9*) was developed so that we can effectively identify materials with high C18:1 content at an early growth stage by marker-assisted selection. Our results may also provide new insight for understanding the complex genetic mechanism of fatty acid metabolism.

Introduction

Oilseed rape (*Brassica napus* L.) is one of the most important oil crops worldwide and provides high-quality edible vegetable oil for human consumption. The edibility and processing quality of rapeseed oil are mainly determined by the fatty acid composition of the seeds, particularly the proportions of the three major unsaturated fatty acids: oleic acid (C18:1), linoleic acid (C18:2) and linolenic acid (C18:3) (Gillingham *et al.*, 2011; Micha and Mozaffarian, 2009). Rapeseed oil with a high C18:1 content and a low C18:3 content is less susceptible to oxidation during storage, frying and food processing and is thus desirable for its thermal stability and long shelf life (Matthäus, 2006; Merrill *et al.*, 2008). Currently, most of the oilseed rape cultivars in the world are of canola quality, that is with low erucic acid and glucosinolate contents and containing approximately 55%–65% oleic acid. One of the major goals for quality breeding of oilseed rape (after the removal of erucic acid) is to further increase the C18:1 content in the seeds. Therefore, identifying high oleic acid germplasm and understanding the genetic control of the trait are the prerequisites for high oleic acid breeding.

A number of quantitative trait loci (QTLs) for C18:1 content have been identified based on linkage (Bao *et al.*, 2018; Burns *et al.*, 2003; Chen *et al.*, 2018; Hu *et al.*, 2006; Smooker *et al.*, 2011; Wen *et al.*, 2015; Yan *et al.*, 2011; Yang *et al.*, 2012b; Zhao *et al.*, 2008) and association (Bao *et al.*, 2018; Körber *et al.*, 2016; Qu *et al.*, 2017) mapping studies. One major QTL located on A5 was detected (Hu *et al.*, 2006; Yang *et al.*, 2012b), and a homologous gene of Arabidopsis *FAD2*, *BnaA.FAD2.a,* was identified as the A5 major QTL (Hu *et al.*, 2006; Yang *et al.*, 2012b). Further analysis indicated that mutated alleles of *BnaA.FAD2.a* on A5 that contained a single-nucleotide substitution (Hu *et al.*, 2006) or a 4-bp insertion (Yang *et al.*, 2012b) in their coding region resulted in an increase in C18:1 content (from 64.1% to 75%). A new mutant of *BnFAD2* with two single-nucleotide polymorphisms (SNPs) in BnFAD2-1 and BnFAD2-2 again confirmed the importance of *FAD2* (Long *et al.*, 2018).

Four orthologues of *FAD2* were identified in *B. napus* in our previous study (Yang *et al.*, 2012b). In contrast to *BnaA.FAD2.b*, three other copies (*BnaA.FAD2.a*, *BnaC.FAD2.a* and *BnaC.FAD2.b*) appear intact and are likely to be functional. Most of the high oleic acid rapeseed germplasm that is currently available results from the mutation of *BnaA.FAD2.a* on A5. Silencing of the *BnFAD2* gene by RNA interference (RNAi) (Peng *et al.*, 2010) or CRISPR/Cas9-mediated genome editing (Okuzaki *et al.*, 2018) or knockout of three functional copies of FAD2 in *B. napus* (Wells *et al.*, 2014) could result in a C18:1 content of up to 84%–85%.

Although great success has been achieved in the development of high oleic acid oilseed rape by manipulating the *FAD2* gene family, the effects of enhanced oleic acid content in seeds on plant growth and development are less clear. Early studies in Arabidopsis showed that the loss-of-function mutant of *FAD2* was hypersensitive to salt stress and low temperature (Miquel, 1994; Miquel *et al.*, 1993; Zhang *et al.*, 2012). The agronomic traits of some oilseed rape plants with an extremely high oleic acid content were also poor when the plants were grown at lower temperatures (Kinney, 1994). Most recently, a field experiment showed that mutant lines with more than 80%

oleate in the seed oil had significantly lower seedling establishment and vigour, delayed flowering and reduced plant height at maturity, and 7%–11% reductions in seed oil content under field conditions (Bai *et al.*, 2018).

It is thus highly desirable to develop novel genetic resources of *B. napus* with both increased C18:1 content and good agronomic performance. In this study, QTL mapping by both linkage and association analyses was performed in *B. napus*, and a novel QTL for C18:1 content was found on chromosome A9, which functions to increase the C18:1 content independently of the *FAD2* gene. By means of fine mapping and gene expression analysis, together with mutant analysis in Arabidopsis, we identified a candidate gene for the locus. Our results thus provide novel information for a better understanding of the genetic architecture of the oleic acid content and fatty acid composition of *B. napus* seeds.

Results

A GWAS identified a novel locus for oleic acid content on chromosome A9

To search for novel loci for fatty acid variant in *B. napus*, we performed a genome-wide association study (GWAS) using a panel of 375 accessions, which were genotyped in our previous study (Liu *et al.*, 2016). All the accessions, which are selected from low erucic acid inbred lines (C22:1 < 3%, Figure 1a), were quantitated by fatty acid profiling. Extensive phenotypic variations in three major unsaturated fatty acids (C18:1, C18:2 and C18:3) were observed among the accessions (Figure 1a). The C18:1 content in the panel exhibited continuous variation, ranging from 48.8% to 76.2%, with an average of 64.7% (Figure 1b). The C18:1 content was significantly associated with the content of most other fatty acids in this low erucic acid association panel, except for the C20:1 content, with a notable high correlation coefficient between the C18:1 and C18:2 contents (−0.92) and between the C18:1 and C18:3 contents (−0.70) (Figure 1c).

Furthermore, a genome-wide association analysis of C18:1 content was conducted with a mixed linear model (PCA + K model). A total of 19 SNPs were significantly associated with C18:1 content with a threshold of $P < 4.32 \times 10^{-5}$ (1/23 168; $-\log_{10}$ (1/23 168) > 4.36) (Figure 1d). Of these significant SNPs, two were detected on A6 and C1, explaining 6.48% and 6.16% of the phenotypic variation, respectively (Figure 1d). The 17 other SNPs were located on A9, and the most significant SNP was Bn-A09-p31549208 ($-\log_{10}(P) = 6.97$), which explained 10.11% of the total phenotypic variation (Figure 1d).

OLEA9 increases oleic content additively with the BnaFad2.a locus

Two *B. napus* inbred lines with significant differences in C18:1 content were used as the parents of the DH population. One line was D126, with a C18:1 content of approximately 75.6%; this line was derived from SW Hickory, which harbours a *fad2* mutation on chromosome A5 (Yang *et al.*, 2012b). The other line was ZP1, with a C18:1 content of approximately 66.1% (Figure 2a). The C18:2 and C18:3 contents of D126 were significantly lower than those of ZP1 (Figure 2a). C18:1, C18:2 and C18:3 accounted for approximately 93% of the total fatty acids in both lines (Figure 2a). For other fatty acids (C16:0, C18:0, C20:1 and C22:1), no significant differences were detected between the two lines (Figure 2a).

In the ZD-DH population, the distribution patterns of the C18:1 content of the three seasons were similar, with nearly a bimodal distribution and a cut-off at 71% for the two groups (Figure 2b), indicating the involvement of a major gene for the trait. However, the two groups did not correspond to exactly a 1:1 ratio across the three seasons. A continuous distribution within the two groups suggested that some minor-effect genes may be involved in the variation.

Since the segregation of oleic acid was not consistent with a single A5 mutation, we aimed to identify other possible loci contributing to the variation. We used a high-density SNP-based genetic map (Wu *et al.*, 2019) for QTL mapping. In total, six QTLs were identified on six chromosomes (A2, A3, A4, A5, A9 and C1) by CIM, each of which explained 1.1%–86.3% of the phenotypic variation (Table 1). Among the QTLs, a major locus with the largest effect, *OLEA5* on A5, was detected, which explained 67.18%, 86.30% and 69.26% of the phenotypic variation during the three seasons. The allele from D126 increased the C18:1 content by 4.88% (additive effect) on average (Table 1; Figure 3a). With the allele-specific marker, *OLEA5* was confirmed to be *BnaA.FAD2.a* (Yang *et al.*, 2012b). In addition to *OLEA5,* another major QTL, *OLEA9,* was detected on A9, which explained 11.25%, 5.72% and 6.29% of the phenotypic variation during the three seasons, and the allele from ZP1 increased the C18:1 content by 2.14% (additive effect) on average (Table 1; Figure 3b). Based on the physical location of the SNP markers in the confidence intervals (bin1751-bin1756) of *OLEA9,* we found that the QTL was located at 27.7–30.1 Mb on chromosome A9 (Figure 3c), which overlapped with the locus detected in GWAS analysis. The remaining four QTLs with minor effects were identified during only one season (Table 1).

To examine the individual or combined effects of *OLEA5* and *OLEA9* on C18:1 content, a closely linked InDel marker, BnA129, located at 27.94 Mb, was developed based on the resequencing data for ZP1 and ZD-12, a DH line from the ZD-DH population with a null *OLEA9* effect (Figure 3d, e). The DH population was then classified into four groups according to the genotypes of the allele-specific marker for *OLEA5* (YQ-fad2a-1) (Yang *et al.*, 2012b) and *OLEA9* (BnA129) (Figure 2d, e). For *OLEA5*, the average C18:1 content in the two groups with the alleles $OLEA5^{BB}OLEA9^{AA}$ or $OLEA5^{BB}OLEA9^{BB}$ was significantly higher than that in the groups with $OLEA5^{AA}OLEA9^{AA}$ or $OLEA5^{AA}OLEA9^{BB}$, with the C18:1 content increased by 9.22%–10.13% (Figure 2f). For *OLEA9*, the average C18:1 content in the two groups with the alleles $OLEA5^{AA}OLEA9^{AA}$ or $OLEA5^{BB}OLEA9^{AA}$ was significantly higher than that in the groups with $OLEA5^{AA}OLEA9^{BB}$ or $OLEA5^{BB}OLEA9^{BB}$, with the C18:1 content increased by 2.35%–3.26% (Figure 3f). The average C18:1 content in the group with both additive-effect alleles ($OLEA5^{BB}OLEA9^{AA}$) was 77.07%, which was 12.48% higher than that in the group without additive-effect alleles ($OLEA5^{AA}OLEA9^{BB}$) (Figure 3f). Our results thus showed that C18:1 can be further increased by integration of *OLEA9* and *OLEA5*.

Fine mapping of OLEA9

For fine mapping of O*LEA9*, we aimed to construct a new bilateral mapping population using two parental lines without the interference of *OLEA5*. One of the two parental lines was ZP1, the original donor of the *OLEA9* locus with a C18:1 content of 66.1%, and the other was ZD12, a DH line from the ZD-DH population with a significantly lower C18:1 content (63.8%). ZD12 shared over 67% similarity with ZP1, as assayed with

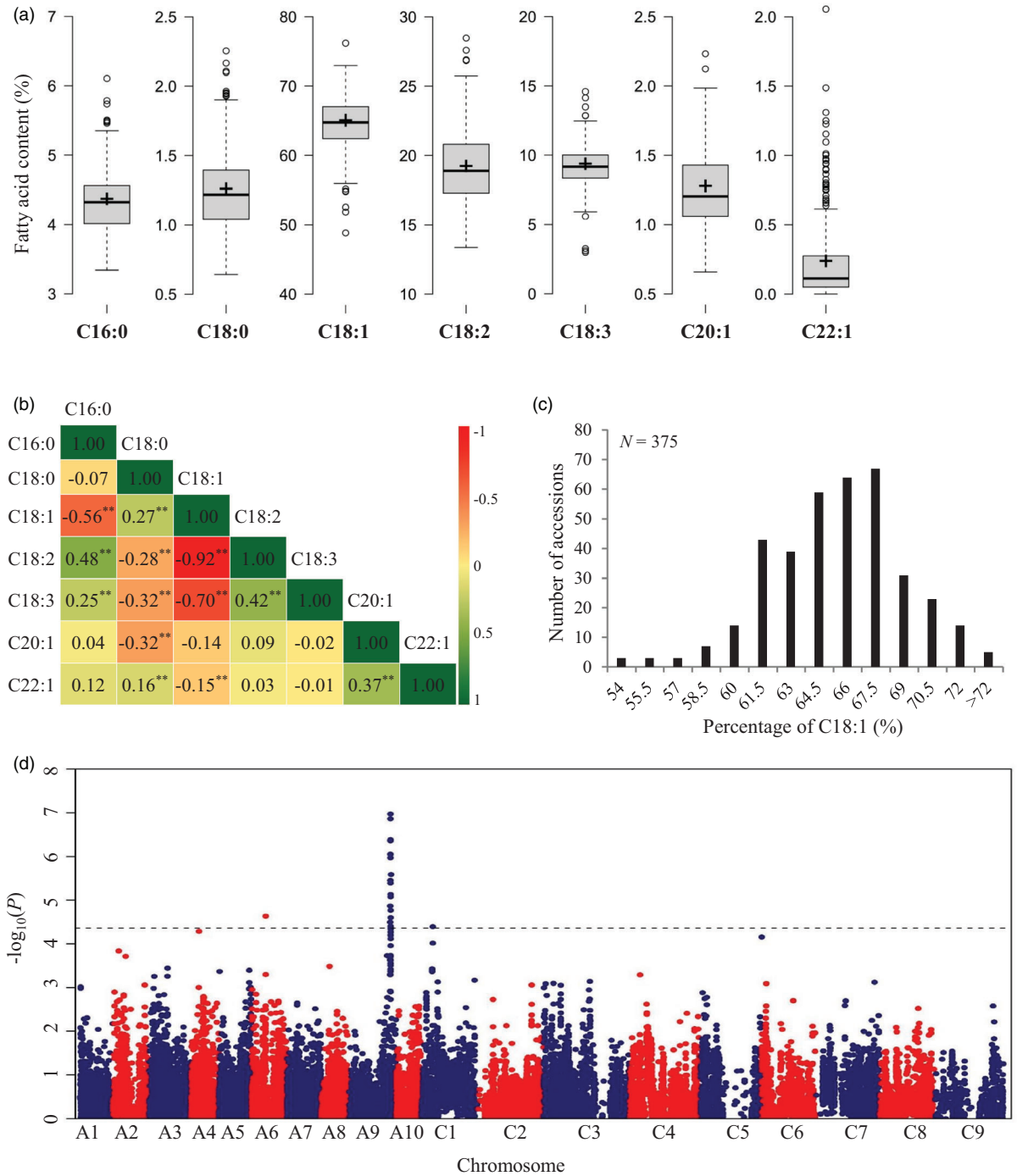

Figure 1 Genome-wide association mapping for oleic acid (C18:1) content using an association panel of 375 *Brassica napus* accessions. (a) Box plot for fatty acid composition of the association panel. The *middle line* indicates the median; the *plus sign* indicates the mean; the *box* indicates the range of the 25–75th percentiles of the total data; the *whiskers* extend 1.5 times the interquartile range from the 25th and 75th percentiles; and the *outer dots* are outliers. (b) Distribution patterns of the C18:1 content in the 375 *B. napus* accessions. (c) Pairwise correlations for fatty acid composition. ** indicates correlations passed significance tests with *P*-values < 0.01. (d) Manhattan plots for the GWAS of C18:1 content. The *dashed horizontal line* depicts the uniform significance threshold ($-\log_{10}1/23\ 168 = 4.36$).

15 622 SNP markers (Figure 4a). In addition to C18:1, the two parental lines also showed differences in C18:2 (Figure 4b). A segregating F2 population (ZD-F2) and backcrossing (ZD-BC) population were then generated for subsequent mapping analysis.

In an F2 subpopulation sampled from the ZD-F2 population, 166 individual plants could be classified into three groups with the marker BnA129, that is homozygous with the parental genotype AA or BB and heterozygous (AB) (Figure 4c). AA and BB exhibited continuous distributions of C18:1 content that

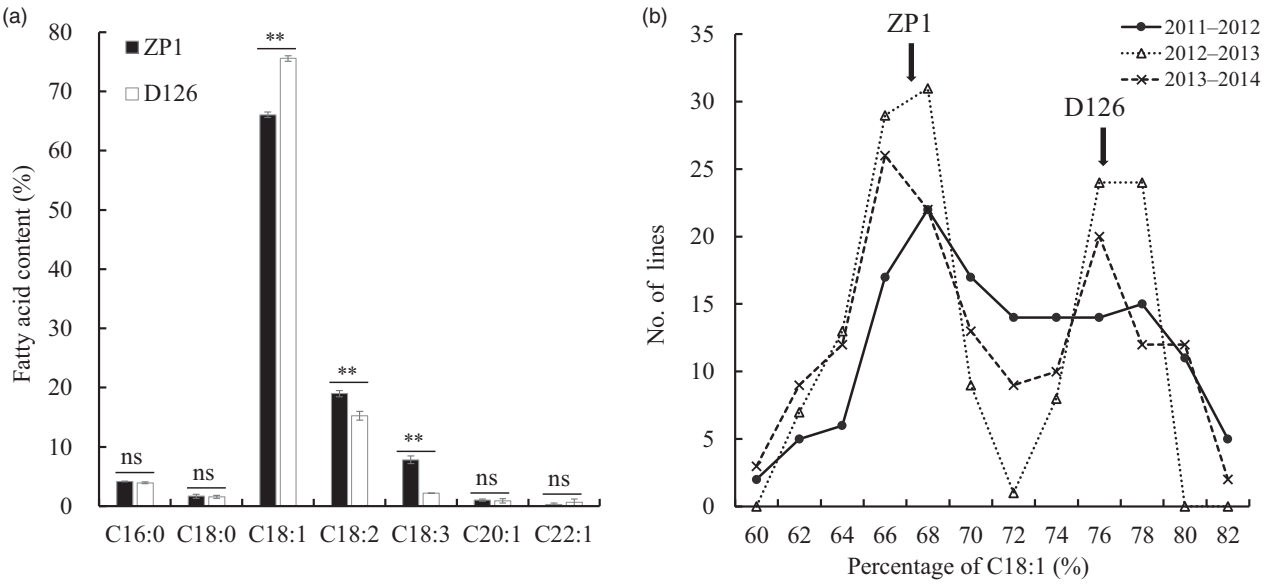

Figure 2 Fatty acid analysis of the two parental lines and the ZD-DH population. (a) Fatty acid composition of the two parental lines ZP1 and D126, including palmitic acid (C16:0), stearic acid (C18:0), oleic acid (C18:1), linoleic acid (C18:2), linolenic acid (C18:3), eicosenoic acid (C20:1) and erucic acid (C22:1). ** indicates a significant difference at the level of $P < 0.01$ (Student's *t*-test), and ns means the difference between the two lines is not statistically significant. (b) Distribution of the C18:1 content of the ZD-DH population measured in three consecutive seasons from 2011 to 2014. Arrows indicate the fatty acid contents of the parental lines (average of three seasons).

Table 1 QTLs for oleic acid (C18:1) content detected in the ZD-DH population

Season	QTL†	Peak‡	LOD§	A	R^2 (%)¶	CI††
2011–2012	*OLEA5*	142.51	45.17	−4.54	67.18	141.7–143.1
	OLEA9	165.71	13.65	1.88	11.25	164.8–166.6
	OLEC1	90.01	4.02	0.92	2.79	85.5–91.6
2012–2013	*OLEA4*	39.61	3.49	0.58	1.10	38.5–42.1
	OLEA5	142.11	75.08	−5.03	86.30	141.6–142.9
	OLEA9	166.51	12.10	3.07	5.72	166.3–167.2
2013–2014	*OLEA2*	93.81	3.82	0.96	1.86	92.4–95.3
	OLEA3	143.01	6.33	−1.09	3.21	142.6–143.4
	OLEA5	142.11	56.19	−5.06	69.26	141.6–143
	OLEA9	167.31	11.44	1.48	6.29	167–168.4

†QTL is nomenclatured as trait name followed by chromosome number.

‡Peak map position (cM) of peak LOD scores.

§A additive effect: positive additivity indicates that the allele from the female parent (ZP1) increases C18:1 content.

¶R^2 proportion for the phenotypic variation explained by the QTL.

††CI Confidence intervals were obtained by marking positions ± 1 LOD from the peak.

overlapped with each other, although the average content for AA (67.63%) was significantly higher than that for BB (64.68%, Figure 4c). The distribution for the AB group was even wider (Figure 4c). With InDel markers newly developed by resequencing the two parental lines, we were able to narrow down the region flanked by BnA144 and BnA153 in the F2 population (Figure S1). These data thus established that *OLEA9* was responsible for the segregation of C18:1 content in the F2 population.

To further pinpoint the locus, we developed a BC3F2 NIL population. A local linkage map consisting of fifteen InDel and SNP markers was subsequently constructed. After three rounds of screening of 5184 BC3F2 individuals with flanking markers, 161 plants with recombination between the markers BnA144 and BnA153 were obtained to pinpoint the region where *OLEA9* was located. SNP markers (Table S3) were developed within the interval of approximately 260 kb between markers BnA144 and BnA153 (Figure 5). Subsequently, these SNP markers, together with previously used markers (BnA129 and BnA153), were employed to genotype 161 BC3F2 individuals and some recombinant progeny of BC3F3 lines. The locus of *OLEA9* was delimited to an interval of approximately 76 kb between SNP1 and SNP7 on the A9 chromosome (Figure 5). Based on the *B. napus* reference genome database (http://www.genoscope.cns.fr/brassicanapus/), twelve genes, designated BnaA09g39470D to BnaA09g39580D, were annotated within this region.

Gene expression analysis of candidate genes

To further pinpoint the candidate genes in the QTL region, we compared the relative gene expression for each of the 12 genes between two NILs (designated H-NIL NIL_{AA} and L-NIL NIL_{BB} for the high and low oleic content lines, respectively) developed from the BC3F2 population. The expression levels of the genes at different stages during seed development were quantified by qPCR. Fold changes between NIL_{AA} and NIL_{BB} were calculated, and a heat map of gene expression was constructed (Figure 6) to illustrate the differences between the NILs for all the candidate genes.

Since BnaA09g39480D and BnaA09g39510D had an average Cq value greater than 33 at all stages, they were regarded as having no expression. Among the remaining ten genes, the expression levels of BnaA09g39520D and BnaA09g39570D were dramatically higher in H-NIL than in L-NIL at almost all developing stages of seeds (except 42 dap), while BnaA09g39490D was

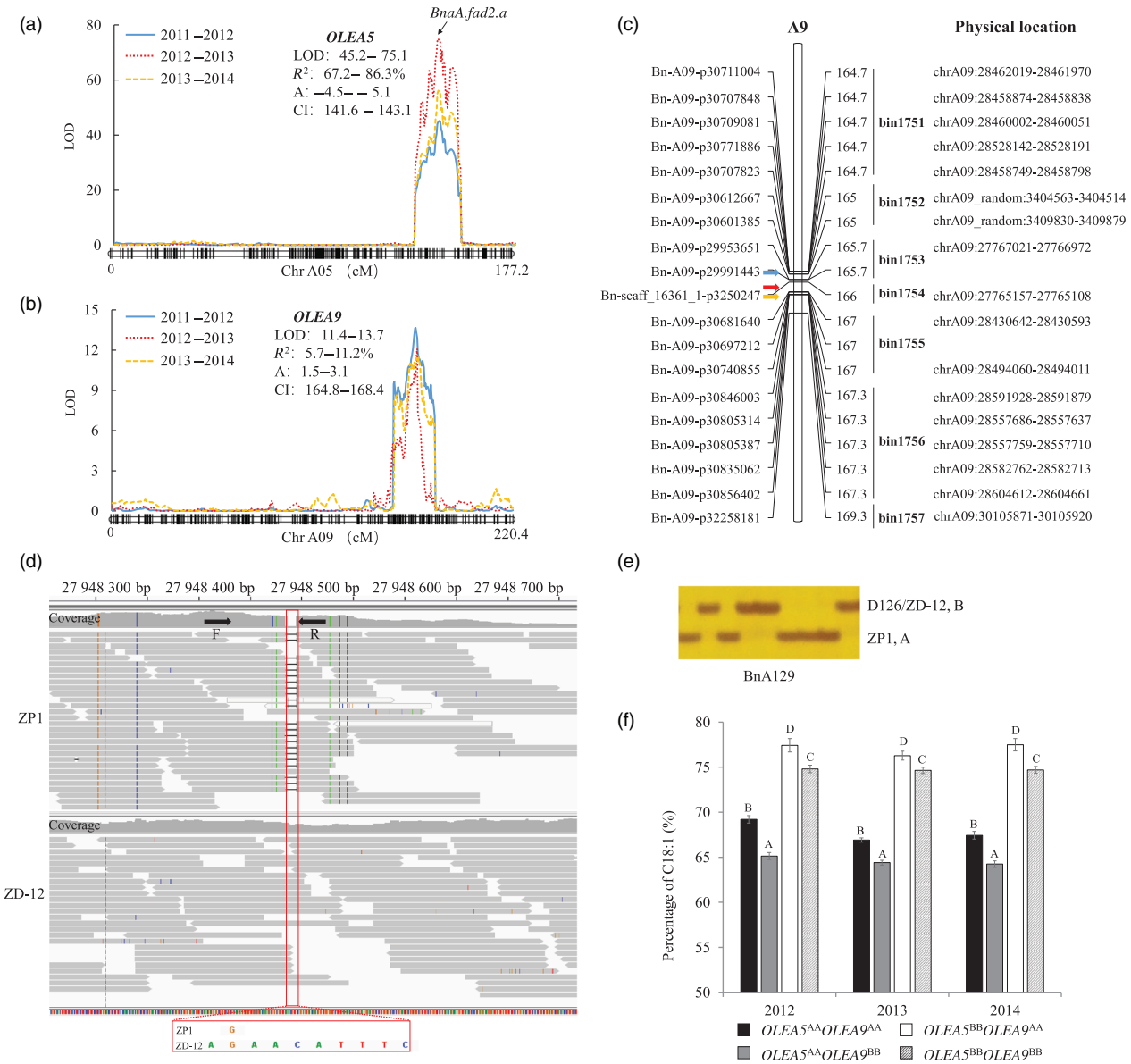

Figure 3 Identification of a novel QTL for oleic acid (C18:1) content on chromosome A9. (a and b) Two major QTLs of *OLEA5* (a) and *OLEA9* (b) were mapped separately. Curves of different colours represent QTL scanned from different seasons. The *BnaA.fad2.a* was responsible for *OLEA5* demonstrated by our previous study (Yang *et al.*, 2012b) and was located on the peak of *OLEA5*. (c) Physical localization of *OLEA9* base on the physical location of the SNP markers in its confidence intervals (bin1751–bin1757). Arrows indicate the peak positions of *OLEA9* detected in three seasons. (d) A closely linked InDel marker BnA129 (at 27.94 Mb) was developed for *OLEA9* according to the resequencing data. The mapping result was displayed by Integrative Genomics Viewer. The red box indicates the positions of InDel. The arrows indicate the forward (F) and reverse (R) primer for BnA129. (e) The PCR-amplified product of BnA129 was separated by 6% denaturing polyacrylamide gels and stained with silver. (f) Effects of individual or combined locus of *OLEA5* and *OLEA9* on C18:1 content in the ZD-DH population as revealed by allelic genotype grouping. Allele-specific marker YQ-fad2a-1 for *OLEA5* (Yang *et al.*, 2012b) and closely linked marker BnA129 for *OLEA9* were used. AA and BB designate the allelic genotype same as parent ZP1 and D126 at a particular locus, respectively. Different uppercase letters indicate significant differences at *P*-values < 0.01.

dramatically lower in H-NIL than in L-NIL (Figure 6). Furthermore, BnaA09g39570D had a much greater fold change between the two NILs ($\log_2$ = 1.46) at 21 dap than at the other stages. The other 7 genes exhibited no significant changes in expression level (Figure 6).

The gene expression differences between H-NIL and L-NIL strongly suggest that oleic acid content is positively correlated with enhanced cand6 (BnaA09g39520D) or cand11 (BnaA09g39570D) or reduced cand3 (BnaA09g39490D) transcript levels. Thus, these three genes are the most likely candidate genes for OLEA9.

To confirm above results, we aligned the sequences with another reference genome of 'ZS11', a Chinese semi-winter *B. napus* (Sun *et al.*, 2017). We compared the genes and their locations in the target region in these two reference genomes against the orthologous region in Arabidopsis. It was found that three more genes are available in ZS11's genome compared with Darmor-bzh. However, two of these three genes are aligned to

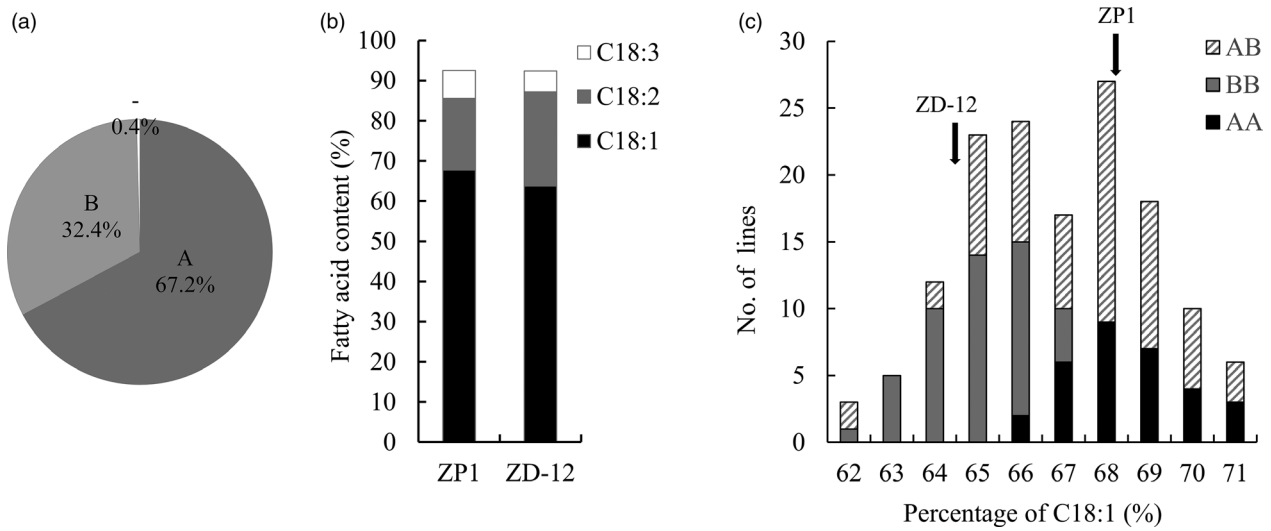

Figure 4 *OLEA9* verification with an F2 population derived from the cross between ZP1 and ZD-12 (a DH line from the ZD-DH population). (a) Genetic background of ZD-12 according to the genotypes of 15 622 SNP markers, 'A': the genotype same as parent line ZP1, 'B': the genotype same as parent line D126, and '−': missing data. (b) The content of three major fatty acids, oleic acid (C18:1), linoleic acid (C18:2) and linolenic acid (C18:3) of the two parental lines ZP1 and ZD-12 in 2015. (c) Distribution patterns of the C18:1 content in a random F2 subpopulation of 166 individuals. Three genotypes (AA, BB and AB) of BnA129 were classified with the marker of BnA129.

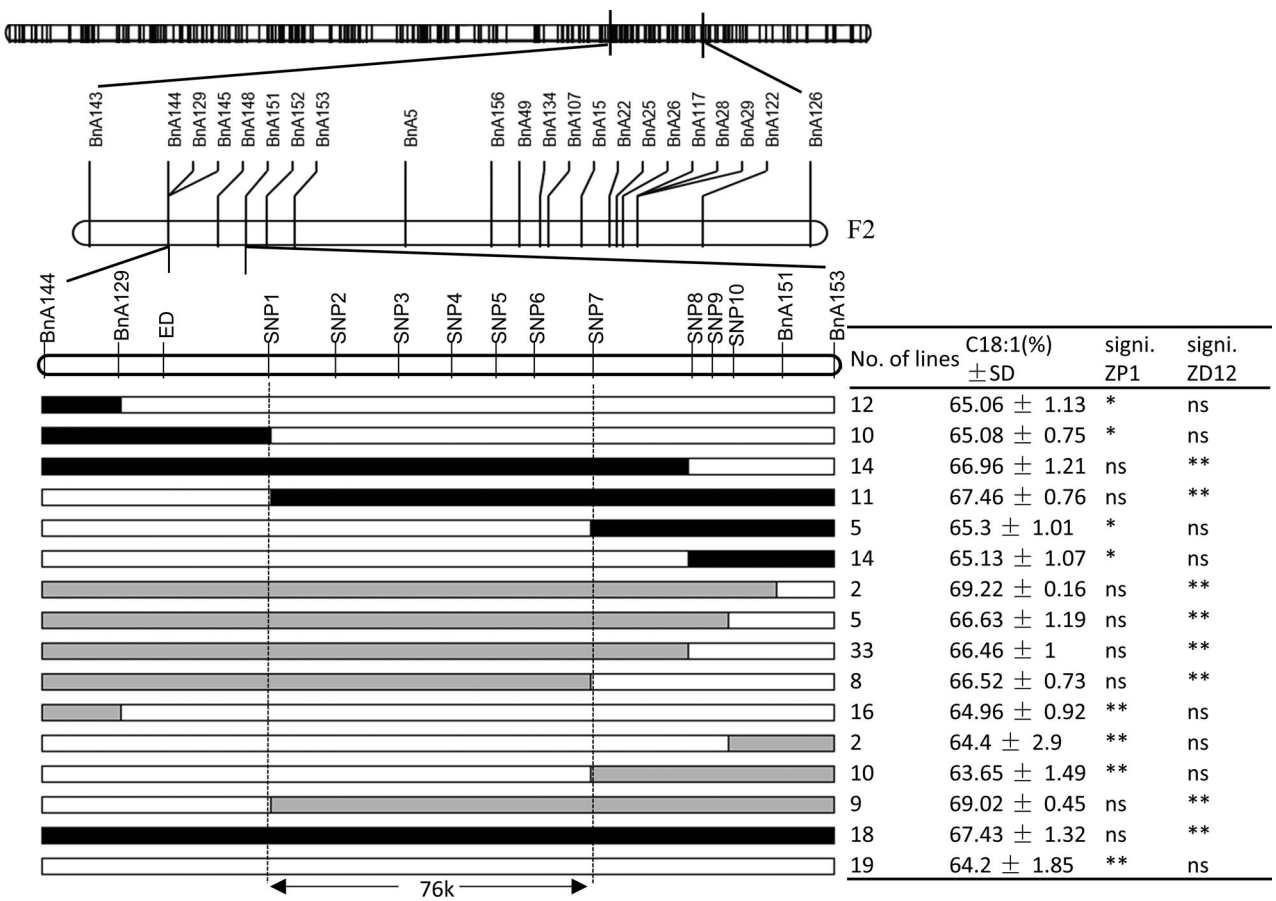

No. of lines	C18:1(%) ±SD	signi. ZP1	signi. ZD12
12	65.06 ± 1.13	*	ns
10	65.08 ± 0.75	*	ns
14	66.96 ± 1.21	ns	**
11	67.46 ± 0.76	ns	**
5	65.3 ± 1.01	*	ns
14	65.13 ± 1.07	*	ns
2	69.22 ± 0.16	ns	**
5	66.63 ± 1.19	ns	**
33	66.46 ± 1	ns	**
8	66.52 ± 0.73	ns	**
16	64.96 ± 0.92	**	ns
2	64.4 ± 2.9	**	ns
10	63.65 ± 1.49	**	ns
9	69.02 ± 0.45	ns	**
18	67.43 ± 1.32	ns	**
19	64.2 ± 1.85	**	ns

Figure 5 Fine mapping of the *OLEA9* loci with a BC_3F_2 segregating population. QTL region was narrowed to 76 kb containing 7 markers (SNP1 to SNP7) using BC3F2 and BC3F3 population. Black box indicates ZP1 genotype, white box indicates ZD12 genotype, and grey box indicates heterozygosis genotype. Statistical significance: $*P < 0.05$; $**P < 0.01$; ns, not significant.

Figure 6 Expression levels of candidate genes in nearly isogenic lines at different stages quantitated by qRT PCR. dap, day after pollination. Gene expression level was calculated by $\log_2$ fold change (number shown) (NIL_{AA}/NIL_{BB}). *X*-axis represents different stages, and *y*-axis represents different gene. Red colour indicates up-regulated change, and green colour indicates down-regulated change.

their Arabidopsis orthologous located on different chromosomes. Another one, although corresponding to an orthologous at the same chromosome, is not on the same orthologous region. Apparently, the distribution of those three genes is not consistent to our QTL mapping results. Therefore, the three genes were ruled out from targeted candidate genes. We supplied the detailed mapping information for the target region in two reference genomes (Table S6).

Verification of the gene in the target region

To infer the potential roles of the candidate genes in determining C18:1 content, we annotated the candidate gene sequences based on the *B. napus* genome (http://www.genoscope.cns.fr/brassicanapus/) and Arabidopsis genome (http://www.arabidopsis.org/). Blast analyses showed that the 12 predicted genes from the *B. napus* reference genome were homologous to 12 genes on *Arabidopsis* chromosome 3 (Table 2). The gene sequence of BnaA09g39570D was highly similar to AT3G62010, which is described as a metal ion-binding protein but without further information. BnaA09g39520D was similar to AT3G61950, which encodes a DNA-binding protein (MYC67) in *A. thaliana*. BnaA09g39490D was annotated as UvrABC system protein, but no more information was given.

Furthermore, Arabidopsis mutants of the three genes were collected (SALK_023939C for AT3G62010), and the fatty acid composition in mature seeds of the mutants was determined. In the *A. thaliana* mutant of AT3G62010 (SALK_023939C), a homolog for BnaA09g39570D, the oleic acid content was significantly higher than that in the other two mutants corresponding to cand6/cand3 and the wild type (Figure 7), suggesting that the BnaA09g39570D gene was most likely the candidate gene within OLEA9. The gene structure and sequence alignment for the two parental lines are displayed in Figure S2.

Discussion

After the successful production of canola-quality oil (low erucic acid and glucosinolate contents), selection for increased C18:1 content and reduced C18:3 content has become one of the most important goals for quality breeding in oilseed rape. To date, most high oleic acid germplasms reported are based on the mutation of *FAD2* genes in Brassica species (Long *et al.*, 2018; Peng *et al.*, 2010; Wells *et al.*, 2014). Such a narrow gene resource may lead to decreased genetic variation and thus compromise the improvement of yield and stress resistance, as illustrated in previous studies (Bai *et al.*, 2018; Dar *et al.*, 2017; Kinney, 1994; Miquel, 1994; Shi *et al.*, 2017). The problem has also been noted in other oil crops, such as peanut and maize (Belo *et al.*, 2008; Janila *et al.*, 2016; Mikkilineni and Rocheford, 2003; Wang *et al.*, 2015, 2018).

In this study, by both QTL mapping and GWAS, we identified a novel QTL (*OLEA9*) for C18:1 content in *B. napus* that further increased the C18:1 content by approximately 3% (Figures 1 and 3). The novel locus can function additively with *fad2* alleles. With further increased oleic content, no negative effects on other traits were observed (Table S1). We had investigated the morphological performance in the NIL lines, and no obvious phenotypic variations other than fatty acid content were observed. For example, the initial flowering dates in the two subpopulations of the NIL were identical (156 days from sowing). It is unlikely that

Table 2 A list of candidate genes and gene annotations in Arabidopsis

	Gene alias	Arabidopsis	ChrA09:position (bp)	Description
cand1	BnaA09g39470D	AT3G61900.1	28000615–28001282	SAUR-like auxin-responsive protein family
cand2	BnaA09g39480D	AT3G61910.1	28004332–28005644	NAC domain protein 66
cand3	BnaA09g39490D	AT3G61920.1	28012722–28013288	–
cand4	BnaA09g39500D	AT3G61930.1	28015922–28016255	–
cand5	BnaA09g39510D	AT3G61940.1	28018344–28019440	Cation efflux family protein
cand6	BnaA09g39520D	AT3G61950.1	28020457–28022135	Basic helix–loop–helix (bHLH) DNA-binding superfamily protein
cand7	BnaA09g39530D	AT3G61960.1	28022399–28025991	Protein kinase superfamily protein
cand8	BnaA09g39540D	AT3G61970.1	28042200–28043079	AP2/B3-like transcriptional factor family protein
cand9	BnaA09g39550D	AT3G61980.1	28046918–28047733	Serine protease inhibitor, Kazal-type family protein
cand10	BnaA09g39560D	AT3G62000.1	28049650–28051588	S-adenosyl-L-methionine-dependent methyltransferases superfamily protein
cand11	BnaA09g39570D	AT3G62010.1	28058343–28064574	–
cand12	BnaA09g39580D	AT3G62020.1	28064637–28065509	Germin-like protein 10

Twelve genes in target region (namely cand1 to cand12 ordered by chromosome position) and their homologous gene in Arabidopsis.

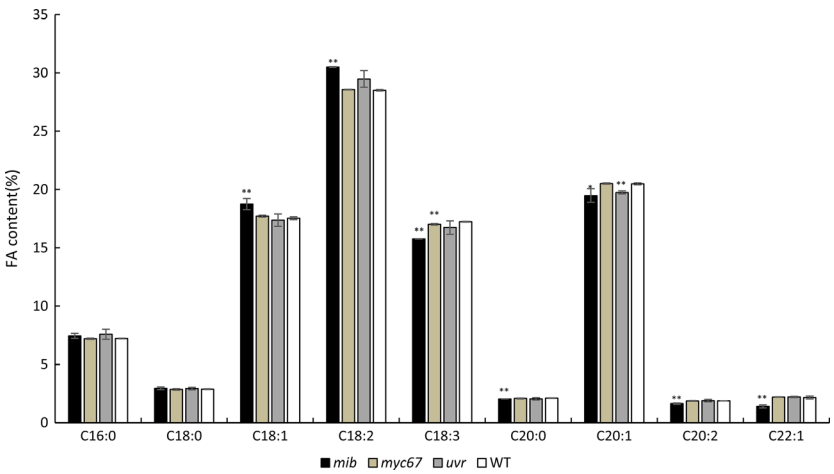

Figure 7 The fatty acid composition of three mutant lines and wild type. *X*-axis shows different fatty acid. *Y*-axis shows the content percentage of each composition. mib/myc67/uvr are three mutants for candidate genes in Arabidopsis. ** represents significance at $P < 0.01$ level and *$P < 0.05$.

the change in fatty acid composition is due to the pleiotropic effects from other processes, such as flowering time or duration, besides fatty acid synthesis. Our finding thus provides a new genetic resource for the manipulation of the oleic acid content in seeds. We further checked the genotypes of the germplasms from China and other countries in GWAS population with the molecular marker ED-1 which was developed in the study (Figure S3) and found that most materials had same genotype with low oleic (lower band in Figure S3). Furthermore, two groups of materials (from China and other countries) showed about similar frequencies of the mutated allele. It is likely that the mutated allele is rare. A further dissection of the molecular mechanism of the gene may uncover other possible pathways involved in fatty acid synthesis in Brassica oilseeds.

Compared with the effect of mutations of *BnFAD2* (on A5), that of *OLEA9* is relatively small. However, the effect is stable, as demonstrated in multiple mapping populations in our study. For example, *OLEA9* explained 5.72%–11.25% of the phenotypic variation in the ZD-DH population during the three seasons (Figure 3 and Table 1). In the ZD-DH population, the additive-effect alleles of *OLEA9* increased the C18:1 content from 64.59% ($OLEA5^{AA}OLEA9^{BB}$) to 67.85% ($OLEA5^{AA}OLEA9^{AA}$) or from 74.72% ($OLEA5^{BB}OLEA9^{BB}$) to 77.07% ($OLEA5^{BB}OLEA9^{AA}$) (Figure 4f). The effects of *OLEA9* were further verified in an F2 population derived from a cross between ZP1 and ZD-12, which had similar genetic backgrounds and a null *OLEA5* effect (Figure 4). The results clearly showed that the locus can be effectively used to further modify the C18:1 content in *B. napus*.

There have been some gene function studies of major QTLs (Liu *et al.*, 2015b; Shi *et al.*, 2019; Xin *et al.*, 2016) in rapeseed since the reference genome was released, but no minor QTLs or genes have been identified for the C18:1 content. Thus, it is challenging to fine-map OLEA9 because of its small effect on the oleic content in *B. napus*, an allotetraploid species with a complex genome and multiple copies of a homologous gene in its two subgenomes (AA and CC). In other crops, such as rice, there have been some minor QTL studies (Deng *et al.*, 2012; Zhang *et al.*, 2016) despite the difficulties in separating minor-effect QTLs. Because of the complexity of the rapeseed genome, gene cloning is difficult for minor QTLs. The detection of minor QTLs is more easily affected by the environment and other errors than that of major QTLs. The desired result can be obtained to some extent only by trying to decrease the effect of background differences in the mapping population or environment and phenotypic error.

Marker-assisted selection (MAS) is an approach for precision plant breeding, and its effectiveness depends on reliable QTLs and closely linked molecular markers. The next-generation sequencing technology offers an unprecedented powerful tool

for developing large numbers of DNA markers, particularly SNP and InDel markers (Varshney *et al.*, 2009; Yang *et al.*, 2012a). InDel markers have become some of the most commonly used markers in plant genetic studies because they are relatively abundant, easy to use, PCR-based and codominant (Păcurar *et al.*, 2012). In this study, we performed resequencing analysis to develop a closely linked InDel marker (BnA129) for *OLEA9* (Figure 3d, e). This marker is very user-friendly because it can be easily distinguished based on the 9 bp differences between ZP1 and ZD-12 (Figure 3d, e). This marker is a reliable, simple and accurate marker for high oleic acid content breeding via MAS in *B. napus*.

At present, it is not clear how the A9 gene increases the C18:1 content in rapeseed. The fatty acid desaturase genes *FAD2* (Miquel, 1992) and *FAD3* (Arondel *et al.*, 1992) are two major genes controlling the C18:1 and C18:3 contents. Strong cosuppression was observed when *FAD2* was overexpressed in the model plant Arabidopsis, and the cosuppression could be overcome in the Arabidopsis rdr6 mutant (Du *et al.*, 2018). Of particular interest, 6% polyunsaturated fatty acids (C18:2 and C18:3) are still produced when the desaturation pathway is completely blocked by FAD2 in *B. napus* (Peng *et al.*, 2010; Wells *et al.*, 2014), suggesting that the remaining C18:2 and C18:3 likely originate from other fatty acid desaturases and/or other types of enzymes.

Based on our mapping results, the region does not harbour any known genes involved in fatty acid metabolism (Li-Beisson *et al.*, 2010). *OLEA9* may participate in a new desaturation pathway that plays a role in subtly fine-tuning fatty acids. Although the candidate gene was annotated as encoding a metal ion-binding protein, little is known about the relationship between fatty acid synthesis and the function of metal ion-binding proteins. Calcium ions play a central role in regulating plant growth, development and adaptation to environmental stresses. Calcium signals are primary regulators of plant growth, development and stress response, and calcium-binding proteins have also been identified as some of the most important components of calcium signal transduction pathways in plants. A pathway (Cav1.1 → CaMKII → NOS) of normal skeletal muscle production in humans regulates the intracellular distribution of the fatty acid transport protein CD36, thus altering fatty acid metabolism. Blocking this pathway results in decreased mitochondrial oxidation and decreased energy expenditure (Georgiou *et al.*, 2015). In plants, Ca^{2+} concentrations, as important classic secondary messengers, can regulate some lipid-related compounds. For example, the activity of plant phospholipase C (PLC), a major membrane phospholipid-hydrolysing enzyme, is regulated by various factors, including Ca^{2+} concentration. The activity of PI-PLC depends on Ca^{2+}, which regulates not only catalytic activity but also the subcellular localization and substrate preference of the enzyme. The PI-PLCs can be translocated between the membrane and cytoplasm, depending on the Ca^{2+} concentrations in cells (Hong *et al.*, 2016; Singh *et al.*, 2015). Moreover, phospholipase Dα1 is the most abundant form of phospholipase D (PLD) in *A. thaliana,* and its activity is characterized by an *in vitro* requirement for millimolar concentrations of Ca^{2+} (Devaiah *et al.*, 2007). The candidate gene might be involved in regulating fatty acid composition by combining Ca^{2+} and thus influencing the relative PLD/PLC participating in the pathway, ultimately changing the fatty acid component. Further gene cloning and functional analysis of *OLEA9* in rapeseed will offer novel information for a more complete understanding of the fatty acid biosynthesis mechanism and provide valuable resources for high oleic acid content breeding in *B. napus*.

Materials and methods

Plant materials

An association panel with 375 rapeseed inbred lines was employed for association analysis of C18:1 content. The accessions were collected from the major breeding institutes across China, and detailed information is provided in Table S4. The association panel was grown in a randomized complete block design with two replicates. Self-pollinated seeds were collected from each replicate for fatty acid profiling.

Two biparental segregating populations were used for primary mapping in this study. The first population was a doubled haploid (DH) population consisting of 150 individual DH lines, referred to as the ZD-DH population. The population was developed from microspore culture of F1 buds of a cross between two *B. napus* inbred lines (ZP1 × D126). The second population was an F2 population derived from a cross between ZP1 and a DH line from the ZD-DH population (ZD-12) with a C18:1 content of approximately 62.71%. The F2 population was designated the ZD-F2 population.

The DH population, along with its parental lines, was grown during three consecutive growing seasons in the years 2011–2012, 2012–2013 and 2013–2014. Self-pollinated seeds were collected from individual DH plants during the season of 2011–2012 or from three plants (one plant from each of three replicates) of each DH line during the seasons of 2012–2013 and 2013–2014 for fatty acid profiling. The field experiments for the DH population followed a complete randomized design with one replicate (2011–2012) or a randomized complete block design with three replicates (2012–2013 and 2013–2014).

The ZD-F2 population, together with its two parental lines, was grown during the 2014–2015 season. One hundred and sixty-six F2 plants were randomly sampled from the F2 population for fatty acid profiling and genotyping.

A BC3F2 population and its derived BC3F3 progenies were constructed (designated ZD-BC) by successive backcrossing using ZD12 (low oleic acid content) as a donor and ZP1 (high oleic acid content) as a recurrent parent followed by self-pollination of F2 individuals, which were grown during the seasons of 2016–2017 and 2017–2018, respectively. Near-isogenic lines (NILs) with high and low oleic acid contents (H-NIL and L-NIL, respectively) were developed. H-NIL accumulated significantly more (~3%–5%) oleic acid than L-NIL (Table S1).

All materials were grown during the winter (the oilseed rape growing season) on the experimental farm of Huazhong Agriculture University, Wuhan, China, and the field management generally followed regular breeding practices.

Wild-type and mutant Arabidopsis plants (Columbia ecotype) were grown in composite soil at 21 °C under a 16-h/8-h day/night photoperiod in a plant growth room. All the T-DNA insertion mutants were verified with LBb, LP and RP primers synthesized with T-DNA Primer Design (http://signal.salk.edu/tdnaprimers.2.html). Table S5 lists the information for the mutants and PCR primers used for mutation verifications.

Phenotypic analysis

Fatty acid profiling of self-pollinated seeds was conducted using gas–liquid chromatography (GC) with a Model 6890 GC analyser (Agilent Technologies, Inc., Wilmington, DE), following the

protocol described by Thies (1971). The individual fatty acid contents were expressed as the percentage of total fatty acids in mature seeds.

Genome-wide association analysis of the oleic acid content in *B. napus*

All the accessions in the association panel were genotyped using 60K SNP array chips as described in Liu *et al.* (2016). For mapping the physical localization of SNP markers, only the top blast hits were considered to be located at a chromosome using an *e*-value threshold of e^{-10}, while blast matches to multiple loci with the same top *e*-value were not considered to be mapped. SNPs that could not be assigned to a *B. napus* chromosome were excluded for further analysis. A total of 23 168 SNPs were retained for further analysis. Principal component analysis (PCA) based on all 23 168 SNPs was performed using the GCTA tool (Yang *et al.*, 2011). A relative kinship matrix of 375 *B. napus* lines was generated using SPAGeDi software (Hardy and Vekemans, 2002). Negative values between two accessions were set to 0. Trait–SNP association was performed using the PCA + K model implemented in TASSEL 4.0 (Bradbury *et al.*, 2007). The significance of the associations between SNPs and the trait was based on a single threshold of $P < 4.32 \times 10^{-5}$ ($P = 1/n$, where n = the number of markers used; $-\log_{10}(1/23\ 168) = 4.36$).

Primary QTL mapping of oleic acid content in the ZD-DH population

The ZD-DH population was genotyped with a 60k SNP array, and a high-density SNP-based genetic map was constructed as previously described (Wu *et al.*, 2019). With the phenotypic data of fatty acids from the DH population, QTL mapping was performed by composite interval mapping (CIM) in QTL Cartographer 2.5 software (http://statgen.ncsu.edu/qtlcart/WQTLCart.htm). A significance threshold for QTLs at the level $P = 0.05$ was determined through permutation analysis using 1000 repetitions. The confidence interval of QTLs was determined by 1-logarithm of the odds (LOD) intervals surrounding the QTL peak. QTLs detected during different seasons were considered the same QTL if they had overlapping confidence intervals. To determine the physical position of SNP markers, SNP probe sequences were used to perform a BlastN (Altschul *et al.*, 1997) search against the *B. napus* 'Darmor-bzh' reference genome (version 4.1) (Chalhoub *et al.*, 2014) with an E-value threshold of 1E-20. Only the top BLAST hits were considered.

Development of InDel and SNP markers through resequencing

High-quality genomic DNA from the parental lines (ZP1 and ZD-12) was subjected to library construction using an Illumina® TruSeq™ DNA Sample Preparation Kit following the manufacturer's instructions. Resequencing was performed with an Illumina HiSeq X Ten sequencer at the Beijing Genomics Institute company to produce paired-end reads that were 2 × 151 bp in length. After acquisition of the raw sequencing data, quality control for raw reads was conducted using the NGS QC Toolkit (Patel and Jain, 2012), including (i) removal of the reads containing primer/adaptor sequences and low-quality reads (the number of bases whose PHRED-like score (*Q*-score) was <20 exceeded 30%), (ii) trimming the first ten base pairs of the reads that showed an unstable base composition, as determined by the percentages of four different nucleotides (A, T, C and G), and the low-quality bases (*Q*-score < 20) from the 3′ end of the reads, and (iii) removal of the reads <50 bp in length. High-quality reads of ZP1 and ZD-12 were then mapped to the *B. napus* 'Darmor-bzh' reference genome (version 4.1) (Chalhoub *et al.*, 2014) by Bowtie 2 v2.2.5 (Langmead and Salzberg, 2012) using the default parameters.

Insertion/deletion (InDel) polymorphism calling was carried out using SAMtools v 0.1.19 (Li *et al.*, 2009) and VarScan v2.3 (Koboldt *et al.*, 2012) with the default parameters. Primers for genome-specific markers were designed using the software Primer 3. Subsequently, these markers were used to screen the parental lines and segregating population, and only the polymorphic markers located within the QTL interval were further employed in the segregating population.

Fine mapping with backcross populations

Genomic DNA was extracted from young leaves of the BC3F2-segregating population consisting of 5184 plants (including the plants for RNA extraction) using the CTAB method. Selected SNPs identified in the target region were confirmed using the Kompetitive Allele-Specific PCR (KASP) method following the instructions from the LGC company (Huang *et al.*, 2017). The QTL position was analysed by examining the genotype of different recombination classes in combination with their phenotypic values. In brief, if the mean oleic acid content for several recombination groups was significantly higher than that of one parent, the QTL was located in the overlapping segment among these recombination groups. Phenotypic and genotypic data analyses were performed using Microsoft Excel.

RNA extraction and qRT-PCR analysis

Individual flowers of the main raceme were tagged on the day of flowering, and developing seeds from two NILs at six developmental stages, namely the ovary and 14, 21, 28, 35 and 42 days after pollination (dap), were collected, immediately frozen in liquid nitrogen and stored at −80 °C for total RNA isolation. Total RNA was extracted using a TransZol Plant Total RNA Extraction Kit (TransGen, Beijing, China) following the manufacturer's instructions. RNA quality (purity and integrity) was monitored by running samples in a 1.0% agarose gel and with an Agilent 2100 Bioanalyzer (Agilent Technologies, Santa Clara, CA, USA). RNA was quantified using a NanoDrop spectrophotometer (Thermo Fisher Scientific, Wilmington, DE, USA). Two genes [BnaC03g45080D (TIP41) and BnaA09g14410D (PP2A-1)] were used as internal controls (Liu *et al.*, 2015a; Wu *et al.*, 2016). Primers were designed based on the reference genome sequences using Primer Premier 5.0 and are listed in Table S2. First-strand cDNA was synthesized from 2 μg RNA per sample using TransScript One-Step gDNA Remover and cDNA Synthesis Kit according to the manufacturer's instructions (TransGen). qRT-PCR was performed using Hieff™ qPCR SYBR Green Master Mix (no ROX) (Yeasen, China) in a Bio-Rad CFX-384 Real-Time PCR System (Bio-Rad, Hercules, CA). Relative expression levels were calculated with LinReg (Ramakers *et al.*, 2003). Data were collected from three biological and two technical replicates, and a heatmap of gene expression level was created with Heatmap Illustrator software (http://hemi.biocuckoo.org/).

Acknowledgements

This work was supported by the National Key Research and Development Program of China (2016YFD0100506-3) and International S&T Cooperation Program of China (2017YFE0104800), Ministry of Science and Technology of China.

Conflict of interest

The authors declare no conflict of interest.

Author contributions

YZ conceived the study. YZ, QZ and JW designed the experiment. QZ and MS performed the experiment. QZ, JW, GC and QY analysed the data. QZ, JW and YZ wrote the manuscript. All authors read and approved the final manuscript.

References

Altschul, S.F., Madden, T.L., Schäffer, A.A., Zhang, J., Zhang, Z., Miller, W. and Lipman, D.J. (1997) Gapped BLAST and PSI-BLAST: a new generation of protein database search programs. *Nucleic Acids Res.* **25**, 3389–3402.

Arondel, V., Lemieux, B., Hwang, I., Gibson, S., Goodman, H.M. and Somerville, C.R. (1992) Map-based cloning of a gene controlling omega-3 fatty acid desaturation in Arabidopsis. *Science*, **258**, 1353–1355.

Bai, S., Engelen, S., Denolf, P., Wallis, J.G., Lynch, K., Bengtsson, J.D., Van Thournout, M. *et al.* (2018) Identification, characterization and field testing of *Brassica napus* mutants producing high-oleic oils. *Plant J.* **98**, 33–41.

Bao, B., Chao, H., Wang, H., Zhao, W., Zhang, L., Raboanatahiry, N., Wang, X. *et al.* (2018) Stable, environmental specific and novel QTL identification as well as genetic dissection of fatty acid metabolism in *Brassica napus*. *Front. Plant Sci.* **9**, 1018.

Belo, A., Zheng, P., Luck, S., Shen, B., Meyer, D.J., Li, B., Tingey, S. *et al.* (2008) Whole genome scan detects an allelic variant of fad2 associated with increased oleic acid levels in maize. *Mol. Genet. Genomics*, **279**, 1–10.

Bradbury, P.J., Zhang, Z., Kroon, D.E., Casstevens, T.M., Ramdoss, Y. and Buckler, E.S. (2007) TASSEL: software for association mapping of complex traits in diverse samples. *Bioinformatics*, **23**, 2633–2635.

Burns, M., Barnes, S., Bowman, J. and Clarke, M. (2003) QTL analysis of an intervarietal set of substitution lines in *Brassica napus*: (i) Seed oil content and fatty acid composition. *Heredity*, **90**, 39.

Chalhoub, B., Denoeud, F., Liu, S., Parkin, I.A., Tang, H., Wang, X., Chiquet, J. *et al.* (2014) Early allopolyploid evolution in the post-neolithic *Brassica napus* oilseed genome. *Science*, **345**, 950–953.

Chen, F., Zhang, W., Yu, K., Sun, L., Gao, J., Zhou, X., Peng, Q. *et al.* (2018) Unconditional and conditional QTL analyses of seed fatty acid composition in *Brassica napus* L. *BMC Plant Biol.* **18**, 49.

Dar, A.A., Choudhury, A.R., Kancharla, P.K. and Arumugam, N. (2017) The FAD2 gene in plants: occurrence, regulation, and role. *Front. Plant Sci.* **8**, 1789.

Deng, H., Liu, H., Li, X., Xiao, J. and Wang, S. (2012) A CCCH-type zinc finger nucleic acid-binding protein quantitatively confers resistance against rice bacterial blight disease. *Plant Physiol.* **158**, 876–889.

Devaiah, S.P., Pan, X., Hong, Y., Roth, M., Welti, R. and Wang, X. (2007) Enhancing seed quality and viability by suppressing phospholipase D in Arabidopsis. *Plant J.* **50**, 950–957.

Du, C., Chen, Y., Wang, K., Yang, Z., Zhao, C., Jia, Q., Taylor, D.C. *et al.* (2018) High-frequency and strong FAD2 co-suppression A bottleneck to increase polyunsaturated fatty acids in seeds. *J. Exp. Bot.* **70**, 985–994.

Georgiou, D.K., Dagnino-Acosta, A., Lee, C.S., Griffin, D.M., Wang, H., Lagor, W.R., Pautler, R.G. *et al.* (2015) Ca2+ binding/permeation via calcium channel, CaV1.1, regulates the intracellular distribution of the fatty acid transport protein, CD36, and fatty acid metabolism. *J. Biol. Chem.* **290**, 23751–23765.

Gillingham, L.G., Harris-Janz, S. and Jones, P.J. (2011) Dietary monounsaturated fatty acids are protective against metabolic syndrome and cardiovascular disease risk factors. *Lipids*, **46**, 209–228.

Hardy, O.J. and Vekemans, X. (2002) SPAGeDi: a versatile computer program to analyse spatial genetic structure at the individual or population levels. *Mol. Ecol. Notes*, **2**, 618–620.

Hong, Y., Zhao, J., Guo, L., Kim, S.C., Deng, X., Wang, G., Zhang, G. *et al.* (2016) Plant phospholipases D and C and their diverse functions in stress responses. *Prog. Lipid Res.* **62**, 55–74.

Hu, X., Sullivan-Gilbert, M., Gupta, M. and Thompson, S.A. (2006) Mapping of the loci controlling oleic and linolenic acid contents and development of fad2 and fad3 allele-specific markers in canola (*Brassica napus* L.). *Theor. Appl. Genet.* **113**, 497–507.

Huang, Z., Peng, G., Liu, X., Deora, A., Falk, K.C., Gossen, B.D., McDonald, M.R. *et al.* (2017) Fine mapping of a clubroot resistance gene in Chinese cabbage using SNP markers identified from bulked segregant RNA sequencing. *Front. Plant Sci.* **8**, 1448.

Janila, P., Pandey, M.K., Shasidhar, Y., Variath, M.T., Sriswathi, M., Khera, P., Manohar, S.S. *et al.* (2016) Molecular breeding for introgression of fatty acid desaturase mutant alleles (ahFAD2A and ahFAD2B) enhances oil quality in high and low oil containing peanut genotypes. *Plant Sci.* **242**, 203–213.

Kinney, A.J. (1994) Genetic modification of the storage lipids of plants. *Curr. Opin. Biotechnol.* **5**, 144–151.

Koboldt, D.C., Zhang, Q., Larson, D.E., Shen, D., McLellan, M.D., Lin, L., Miller, C.A. *et al.* (2012) VarScan 2: somatic mutation and copy number alteration discovery in cancer by exome sequencing. *Genome Res.* **22**, 568–576.

Körber, N., Bus, A., Li, J., Parkin, I.A., Wittkop, B., Snowdon, R.J. and Stich, B. (2016) Agronomic and seed quality traits dissected by genome-wide association mapping in *Brassica napus*. *Front. Plant Sci.* **7**, 386.

Langmead, B. and Salzberg, S.L. (2012) Fast gapped-read alignment with Bowtie 2. *Nat. Methods*, **9**, 357–359.

Li, H., Handsaker, B., Wysoker, A., Fennell, T., Ruan, J., Homer, N., Marth, G. *et al.* (2009) The sequence alignment/map format and SAMtools. *Bioinformatics*, **25**, 2078–2079.

Li-Beisson, Y., Shorrosh, B., Beisson, F., Andersson, M.X., Arondel, V., Bates, P.D., Baud, S. *et al.* (2010) Acyl-Lipid Metabolism. *Arabidopsis Book*, **8**, e0133.

Liu, H., Yang, Q., Fan, C., Zhao, X., Wang, X. and Zhou, Y. (2015a) Transcriptomic basis of functional difference and coordination between seeds and the silique wall of *Brassica napus* during the seed-filling stage. *Plant Sci.* **233**, 186–199.

Liu, J., Hua, W., Hu, Z., Yang, H., Zhang, L., Li, R., Deng, L. *et al.* (2015b) Natural variation in ARF18 gene simultaneously affects seed weight and silique length in polyploid rapeseed. *Proc. Natl Acad. Sci. USA*, **112**, E5123–E5132.

Liu, S., Fan, C., Li, J., Cai, G., Yang, Q., Wu, J., Yi, X. *et al.* (2016) A genome-wide association study reveals novel elite allelic variations in seed oil content of *Brassica napus*. *Theor. Appl. Genet.* **129**, 1203–1215.

Long, W., Hu, M., Gao, J., Chen, S., Zhang, J., Cheng, L. and Pu, H. (2018) Identification and functional analysis of two new mutant BnFAD2 alleles that confer elevated oleic acid content in rapeseed. *Front. Genet.* **9**, 399.

Matthäus, B. (2006) Utilization of high-oleic rapeseed oil for deep-fat frying of French fries compared to other commonly used edible oils. *Eur. J. Lipid Sci. Technol.* **108**, 200–211.

Merrill, L.I., Pike, O.A., Ogden, L.V. and Dunn, M.L. (2008) Oxidative stability of conventional and high-oleic vegetable oils with added antioxidants. *J. Am. Oil Chem.' Soc.* **85**, 771–776.

Micha, R. and Mozaffarian, D. (2009) Trans fatty acids: effects on metabolic syndrome, heart disease and diabetes. *Nat. Rev. Endocrinol.* **5**, 335–344.

Mikkilineni, V. and Rocheford, T.R. (2003) Sequence variation and genomic organization of fatty acid desaturase-2 (fad2) and fatty acid desaturase-6 (fad6) cDNAs in maize. *Theor. Appl. Genet.* **106**, 1326–1332.

Miquel, M. (1992) Arabidopsis mutants deficient in polyunsaturated fatty acid synthesis. Biochemical and genetic characterization of a plant oleoyl-phosphatidylcholine desaturase. *J. Biol. Chem.* **267**, 1502–1509.

Miquel, M.F. (1994) High-oleate oilseeds fail to develop at low temperature. *Plant Physiol.* **106**, 421–427.

Miquel, M., James, D. and Dooner, H. (1993) Arabidopsis requires polyunsaturated lipids for low-temperature survival. *Proc. Natl Acad. Sci.* **90**, 6208–6212.

Okuzaki, A., Ogawa, T., Koizuka, C., Kaneko, K., Inaba, M., Imamura, J. and Koizuka, N. (2018) CRISPR/Cas9-mediated genome editing of the fatty acid desaturase 2 gene in *Brassica napus*. *Plant Physiol. Biochem.* **131**, 63–69.

Păcurar, D.I., Păcurar, M.L., Street, N., Bussell, J.D., Pop, T.I., Gutierrez, L. and Bellini, C. (2012) A collection of INDEL markers for map-based cloning in seven Arabidopsis accessions. *J. Exp. Bot.* **63**, 2491–2501.

Patel, R.K. and Jain, M. (2012) NGS QC toolkit: a toolkit for quality control of next generation sequencing data. *PLoS ONE*, **7**, e30619.

Peng, Q., Hu, Y., Wei, R., Zhang, Y., Guan, C., Ruan, Y. and Liu, C. (2010) Simultaneous silencing of FAD2 and FAE1 genes affects both oleic acid and erucic acid contents in *Brassica napus* seeds. *Plant Cell Rep.* **29**, 317–325.

Qu, C., Jia, L., Fu, F., Zhao, H., Lu, K., Wei, L., Xu, X. *et al.* (2017) Genome-wide association mapping and Identification of candidate genes for fatty acid composition in *Brassica napus* L. using SNP markers. *BMC Genom.* **18**, 232.

Ramakers, C., Ruijter, J.M., Deprez, R.H.L. and Moorman, A.F.M. (2003) Assumption-free analysis of quantitative real-time polymerase chain reaction (PCR) data. *Neurosci. Lett.* **339**, 62–66.

Shi, J., Lang, C., Wang, F., Wu, X., Liu, R., Zheng, T., Zhang, D. *et al.* (2017) Depressed expression of FAE1 and FAD2 genes modifies fatty acid profiles and storage compounds accumulation in *Brassica napus* seeds. *Plant Sci.* **263**, 177–182.

Shi, L., Song, J., Guo, C., Wang, B., Guan, Z., Yang, P., Chen, X. *et al.* (2019) A CACTA-like transposable element in the upstream region of BnaA9.CYP78A9 acts as an enhancer to increase silique length and seed weight in rapeseed. *Plant J.* **98**, 524–539.

Singh, A., Bhatnagar, N., Pandey, A. and Pandey, G.K. (2015) Plant phospholipase C family: regulation and functional role in lipid signaling. *Cell Calcium*, **58**, 139–146.

Smooker, A.M., Wells, R., Morgan, C., Beaudoin, F., Cho, K., Fraser, F. and Bancroft, I. (2011) The identification and mapping of candidate genes and QTL involved in the fatty acid desaturation pathway in *Brassica napus*. *Theor. Appl. Genet.* **122**, 1075–1090.

Sun, F., Fan, G., Hu, Q., Zhou, Y., Guan, M., Tong, C., Li, J. *et al.* (2017) The high-quality genome of *Brassica napus* cultivar 'ZS11' reveals the introgression history in semi-winter morphotype. *Plant J.* **92**, 452–468.

Thies, W. (1971) *Schnelle und einfache Analysen der Fettsaurezusammensetzung in einzelnen Raps-Kotyledonen. I. Gaschromatographische und papierchromatographische Methoden. Z Pflanzenzucht* **65**, 181–202.

Varshney, R.K., Nayak, S.N., May, G.D. and Jackson, S.A. (2009) Next-generation sequencing technologies and their implications for crop genetics and breeding. *Trends Biotechnol.* **27**, 522–530.

Wang, M.L., Khera, P., Pandey, M.K., Wang, H., Qiao, L., Feng, S., Tonnis, B. *et al.* (2015) Genetic mapping of QTLs controlling fatty acids provided insights into the genetic control of fatty acid synthesis pathway in peanut (*Arachis hypogaea* L.). *PLoS ONE*, **10**, e0119454.

Wang, M.L., Chen, C.Y., Tonnis, B., Pinnow, D., Davis, J., An, Y.C. and Dang, P. (2018) Changes of seed weight, fatty acid composition, and oil and protein contents from different peanut FAD2 genotypes at different seed developmental and maturation stages. *J. Agric. Food Chem.* **66**, 3658–3665.

Wells, R., Trick, M., Soumpourou, E., Clissold, L., Morgan, C., Werner, P., Gibbard, C. *et al.* (2014) The control of seed oil polyunsaturate content in the polyploid crop species *Brassica napus*. *Mol. Breed.* **33**, 349–362.

Wen, J., Xu, J., Long, Y., Xu, H., Wu, J., Meng, J. and Shi, C. (2015) Mapping QTLs controlling beneficial fatty acids based on the embryo and maternal plant genomes in *Brassica napus* L. *J. Am. Oil Chem.' Soc.* **92**, 541–552.

Wu, J., Zhao, Q., Yang, Q., Liu, H., Li, Q., Yi, X., Cheng, Y. *et al.* (2016) Comparative transcriptomic analysis uncovers the complex genetic network for resistance to Sclerotinia sclerotiorum in *Brassica napus*. *Sci. Rep.* **6**, 19007.

Wu, J., Chen, P., Zhao, Q., Cai, G., Hu, Y., Xiang, Y., Yang, Q. *et al.* (2019) Co-location of QTL for Sclerotinia stem rot resistance and flowering time in *Brassica napus*. *Crop J.* **7**, 227–237.

Xin, Q., Shen, Y., Li, X., Lu, W., Wang, X., Han, X., Dong, F. *et al.* (2016) MS5 mediates early meiotic progression and its natural variants may have applications for hybrid production in *Brassica napus*. *Plant Cell*, **28**, 1263–1278.

Yan, X.Y., Li, J.N., Wang, R., Jin, M.Y., Chen, L., Qian, W., Wang, X.N. *et al.* (2011) Mapping of QTLs controlling content of fatty acid composition in rapeseed (*Brassica napus*). *Genes Genom.* **33**, 365–371.

Yang, J., Lee, S.H., Goddard, M.E. and Visscher, P.M. (2011) GCTA: a tool for genome-wide complex trait analysis. *Am. J. Hum. Genet.* **88**, 76–82.

Yang, H., Tao, Y., Zheng, Z., Li, C., Sweetingham, M.W. and Howieson, J.G. (2012a) Application of next-generation sequencing for rapid marker development in molecular plant breeding: a case study on anthracnose disease resistance in *Lupinus angustifolius* L. *BMC Genom.* **13**, 318.

Yang, Q., Fan, C., Guo, Z., Qin, J., Wu, J., Li, Q., Fu, T. *et al.* (2012b) Identification of FAD2 and FAD3 genes in *Brassica napus* genome and development of allele-specific markers for high oleic and low linolenic acid contents. *Theor. Appl. Genet.* **125**, 715–729.

Zhang, J., Liu, H., Sun, J., Li, B., Zhu, Q., Chen, S. and Zhang, H. (2012) Arabidopsis fatty acid desaturase FAD2 is required for salt tolerance during seed germination and early seedling growth. *PLoS ONE*, **7**, e30355.

Zhang, H.W., Fan, Y.Y., Zhu, Y.J., Chen, J.Y., Yu, S.B. and Zhuang, J.Y. (2016) Dissection of the qTGW1.1 region into two tightly-linked minor QTLs having stable effects for grain weight in rice. *BMC Genet.* **17**, 98.

Zhao, J., Dimov, Z., Becker, H.C., Ecke, W. and Möllers, C. (2008) Mapping QTL controlling fatty acid composition in a doubled haploid rapeseed population segregating for oil content. *Mol. Breed.* **21**, 115–125.

Supporting information

Additional supporting information may be found online in the Supporting Information section at the end of the article.

Figure S1 Genetic linkage map constructed by F2 population.
Figure S2 Gene structure and sequence alignment with IGV software.
Figure S3 Genotyping of partial germplasms from the GWAS population. (a) Germplasms from other countries than China. (b) Germplasms from China randomly sampled from the population.
Table S1 Seed fatty acid composition (%), oil content (%) and thousand seed weight (TSW) of NIL lines.
Table S2 Primer list for qRT PCR.
Table S3 InDel and KASP primer sequences in the *OLEA9* target region.
Table S4 Detailed information for 375 rapeseed inbred lines employed for association analysis.
Table S5 Primer sequences for checking Arabidopsis mutant lines.
Table S6 Gene information in target region by using two reference genomes.

